

Epilepsy surgery: Evaluating robustness using dynamic network models

Junges, Leandro; Woldman, Wessel; Benjamin, Oscar; Terry, John

Citation for published version (Harvard):

Junges, L, Woldman, W, Benjamin, O & Terry, J 2020, 'Epilepsy surgery: Evaluating robustness using dynamic network models', *Chaos*, vol. 30, no. 113106.

[Link to publication on Research at Birmingham portal](#)

General rights

Unless a licence is specified above, all rights (including copyright and moral rights) in this document are retained by the authors and/or the copyright holders. The express permission of the copyright holder must be obtained for any use of this material other than for purposes permitted by law.

- Users may freely distribute the URL that is used to identify this publication.
- Users may download and/or print one copy of the publication from the University of Birmingham research portal for the purpose of private study or non-commercial research.
- User may use extracts from the document in line with the concept of 'fair dealing' under the Copyright, Designs and Patents Act 1988 (?)
- Users may not further distribute the material nor use it for the purposes of commercial gain.

Where a licence is displayed above, please note the terms and conditions of the licence govern your use of this document.

When citing, please reference the published version.

Take down policy

While the University of Birmingham exercises care and attention in making items available there are rare occasions when an item has been uploaded in error or has been deemed to be commercially or otherwise sensitive.

If you believe that this is the case for this document, please contact UBIRA@lists.bham.ac.uk providing details and we will remove access to the work immediately and investigate.

Epilepsy Surgery: Evaluating robustness using dynamic network models

Leandro Junges^{1,2,*,a}, Wessel Woldman^{1,2,*}, Oscar J. Benjamin³, John R. Terry^{1,2}

Affiliations

¹ Centre for Systems Modelling and Quantitative Biomedicine, University of Birmingham, Birmingham, B15 2TT, United Kingdom.

² Institute for Metabolism and Systems Research, University of Birmingham, Birmingham, B15 2TT, United Kingdom.

³ Department of Engineering Mathematics, University of Bristol, Bristol, BS8 1UB United Kingdom.

* Denotes equal contribution as first author.

^a Corresponding author: l.junges@bham.ac.uk.

Abstract

Epilepsy is one of the most common neurological conditions, affecting over 65 million people worldwide. Over one third of people with epilepsy are considered refractory: they do not respond to drug treatment. For this significant cohort of people, surgery is a potentially transformative treatment. However, only a small minority of people with refractory epilepsy are considered suitable for surgery and long-term seizure freedom is only achieved in one half of cases. Recently, several computational approaches have been proposed to support presurgical planning. Typically, these approaches use a dynamic network model to explore the potential impact of a surgical resection *in silico*. The network component of the model is informed by clinical imaging data and is considered static thereafter. This assumption critically overlooks the plasticity of the brain and therefore how continued evolution of the brain network post-surgery may impact upon the success of a resection in the longer term. In this work, we use a simplified dynamic network model, that describes transitions to seizures, to systematically explore how network structure influences seizure propensity, both before and after virtual resections. We illustrate key results in small networks, before extending our findings to larger networks. We demonstrate how evolution of brain networks post resection can result in a return to increased seizure propensity. Our results effectively determine the robustness of a given resection to network reconfiguration and so provide a potential strategy for optimising long-term seizure freedom.

Brain surgery is a potentially life-changing treatment for people with epilepsy that do not respond to drug therapy. Unfortunately, identifying brain regions responsible for seizure generation and spread is complex and so the number of people considered suitable for surgery is relatively low and outcomes are non-optimal. Many people for whom surgery appears initially successful see seizures return within a year or so. Several computational methods that combine network analysis and mathematical modelling have been proposed lately to support surgical planning by evaluating virtually the potential impacts of a surgical resection. In such models, representations of brain networks are extracted from clinical data. However, these methods typically consider brain networks to be static after surgery, ignoring the potential effects of network reorganization in long-term seizure freedom. In this work we use a dynamic network model of seizure transition to systematically evaluate the influence of network structure in seizure propensity before and after virtual resections. We use small networks to illustrate how a successful resection can be adversely influenced by post-surgical network reconfiguration, where the creation or destruction of network edges lead to an increase in seizure propensity. We then

51 extend our results to networks with sizes more in line with what is typically obtained from
52 clinical data. The results presented in this work shed light upon the issue of brain networks
53 sensitivity to reconfiguration, and provide a framework to evaluate the robustness of therapeutic
54 interventions. This framework can potentially be used more generally to explore robustness in
55 the behaviour of dynamic coupled systems.

58 I. Introduction

59
60 Epilepsy is a very common serious primary neurological condition¹. Epilepsy is characterised by the
61 tendency to have spontaneous seizures². In some cases, the cause of seizures is readily apparent (e.g.
62 a brain tumour or cortical lesion), however for the majority the definitive cause is unknown. With
63 appropriate treatment, approaching two-thirds of people with epilepsy have well-controlled seizures³.
64 For the remaining third, more invasive therapies including electrical stimulation⁴ and surgery⁵ are
65 potential options. For those people with epilepsy for whom surgery is considered appropriate, long-
66 term seizure freedom is achieved in around 50% of cases. However, success rates may be as high as
67 80% where an affected brain region is clearly identifiable, but as low as 15% in cases
68 where no such brain region is apparent⁶. A further consideration is the lasting impact of the surgery.
69 Many people with epilepsy display a reduction in seizure rates immediately after surgery, however
70 their seizures often return over time and may be different in nature to those with which they were
71 initially diagnosed^{6,7}. Despite these challenges, epilepsy surgery has been shown to be a highly cost-
72 effective solution⁸ and many believe it should gain more widespread acceptance as an alternative
73 treatment for people with refractory epilepsy^{9,10}.

74
75 One explanation for this wide variation in surgery success rates is the role of large-scale brain
76 networks in seizure generation, which has become increasingly recognised in recent years¹¹⁻¹⁶. This
77 recognition has resulted in the International League Against Epilepsy updating its operational
78 classification of seizure types to reflect the role networks play in the generation of
79 seizures¹⁷. Clinically, brain networks can be characterised through structural or functional
80 relationships. Structural connections essentially represent the anatomical links between brain regions
81 as typically measured using magnetic resonance imaging (MRI). These structural links are
82 hypothesised to form the basis of functional connections between brain areas. Typically, functional
83 connections are inferred statistically from time-series data such as functional MRI,
84 electroencephalography (EEG), or magnetoencephalography (MEG) (see Stam¹⁸ for a comprehensive
85 review).

86
87 However, as van Mierlo and colleagues observed¹⁶: “*With the growing enthusiasm for connectivity it*
88 *is often overlooked that in reality, all we have are statistical interdependencies of signals, which*
89 *should be interpreted cautiously.*” Because of the largely qualitative nature of these clinically defined
90 networks, there has been considerable interest in the development and application of mathematical
91 methods, notably from network science and dynamical systems, to better understand seizure
92 generation and therefore the condition of epilepsy¹⁹. For example, in early work²⁰ a dynamic network
93 model was constructed to demonstrate that emergent activity characteristic of different seizure
94 types could arise due to changes in either the edge structure of the network, or the dynamic activity
95 within nodes. The dynamics within each node of this model are determined by a bistable switch that
96 characterises transitions between phenomenological representations of healthy (background) and
97 pathological (seizure) states. Based upon the normal form of a sub-critical Hopf bifurcation, this class
98 of model was first introduced in the context of epilepsy by Kalitzin *et al.*²¹ and Benjamin *et al.*²².
99 Although a gross simplification of the brain, the model provided insight as to why loss of connections
100 between brain regions made the brain – on average – more seizure prone. Many subsequent approaches

101 have since built on this concept of seizures as an emergent property of the interplay between nodes
102 within a network and its connectivity (see Milton²³ for a classical introduction and Moraes *et al.*²⁴ for
103 a recent review).

104

105 A number of approaches have recently been developed that combine clinical data with mathematical
106 models to understand surgical strategies or to inform pre-surgical planning. For example, a
107 computational study²⁵ identified differences between structural brain networks of people with
108 temporal lobe epilepsies and healthy controls. They further showed that measures of seizure rates (as
109 calculated from the model) could be lowered by removing certain nodes within
110 the network. In 2016, Goodfellow *et al.*²⁶, undertook the first study that utilised intracranial EEG
111 (iEEG) recordings, alongside pre- and post-operative imaging, to predict *in silico* the effects of
112 removing macroscopic regions of the cortex in the emergence of epileptiform activity. Key findings
113 of this study were replicated using a bistable dynamic network model in work by Sinha *et al.*²⁷.
114 Khambhati *et al.*²⁸ simulated cortical resections in virtual brain networks obtained from
115 electrocorticography, and suggested a *push-pull* control effect resulting from a competition between
116 synchronizing and desynchronizing network regions which influence seizure spread. Jirsa *et al.*²⁹ have
117 developed a computational approach to support brain surgery based on non-invasive structural data
118 (the *Virtual Epileptic Patient*). Lopes *et al.*³⁰ used iEEG recordings to show that scale-free and rich-
119 club functional brain networks have specific nodes that are central for seizure generation and,
120 therefore, should be targeted in resective surgery.

121

122 Whilst these approaches have shown promise, it is very important to consider the implications of the
123 assumptions underlying both epilepsy surgery and the models with which predictions of outcome are
124 made. One critical assumption is that the perturbation to the brain as a consequence of the surgery is
125 ever lasting. However, there is no reason to assume that connections between remaining regions of the
126 brain stay static post-surgery. On the contrary, the brain is highly plastic³¹ and evidence of ongoing
127 changes are supported by the clinical observations of declining seizure freedom over time in people
128 who have undergone apparently successful surgery^{6,7}. A further challenge is that we do not know *a*
129 *priori* how best to mathematically characterise brain dynamics that underpin the emergence of seizures
130 within a dynamic network. Recent work³² has demonstrated that predictions of the outcome of surgical
131 strategies may depend on the choice of mathematical model that defines the behaviour of each node
132 within the network.

133

134 Collectively these issues relate to dynamic robustness. By this we mean how do ongoing dynamic
135 factors impact upon the choice of perturbation that we might make. This is an important consideration
136 in the context of epilepsy surgery. For example, there may be multiple routes to achieving apparent
137 seizure freedom, however some may be more dynamically robust than others. In this work we evaluate
138 how network topology influences seizure propensity, and quantify the effects of virtual surgical
139 resection, represented by the removal of network nodes. Finally, the results are extended to larger
140 networks, more in line with measures obtained from clinical data.

141

142 **II. Methods**

143

144 **A. Dynamic Network Model**

145

146 We consider a bistable dynamic network model that can generate both healthy background-like and
147 seizure-like activity at a phenomenological level^{21,22}. Activity within each brain region is described by
148 a modified version of the normal form of the subcritical Hopf bifurcation, with an additional equation
149 to describe slow variations of the “excitability” variable λ ^{22,33}:

150

151
$$\frac{dz_j}{dt} = z_j(\lambda_j - 1 + i\omega + 2|z_j|^2 - |z_j|^4) + \frac{\beta}{N} \sum_{k=1}^N A_{kj}(z_k - z_j) + \alpha dW_j \quad (1)$$

152
$$\tau \frac{d\lambda_j}{dt} = \lambda_{j0} - \lambda_j - |z_j|^2 \quad (2)$$

153
 154 where $j = 1, \dots, N$ represent the network nodes. These coupled stochastic differential equations
 155 describe the evolution of complex variables z , where the coupling is linear and proportional to the
 156 difference between node states. The real part of the state variables can be thought of as a proxy of the
 157 electrographic activity of a brain region, for example as measured using EEG. In this framework,
 158 network nodes are associated to regions of the brain generating the electrical signal measured by the
 159 EEG electrodes. When $\lambda_j \in [0,1]$, there are two distinct dynamical behaviour: low-amplitude noisy
 160 activity near the origin (stable fixed point $z = 0$) and large amplitude, oscillations (stable limit cycle
 161 at $|z|^2 = 1 + \sqrt{\lambda}$). These two stable attractors are separated by an unstable limit cycle (located at
 162 $|z|^2 = 1 - \sqrt{\lambda}$). At a phenomenological level, the stable fixed point can be thought of as “background-
 163 like” activity as observed in electrographic recordings, whereas the stable limit cycle corresponds to
 164 “seizure-like” activity. For large enough noise, the system will eventually transition into the seizure-
 165 like state, after which the slow variable decreases (past the limit point located at 0) and the system will
 166 return back (with time-scale τ) to the background-like state.

167
 168 Consequently, this phenomenological model provides a framework in which one can systematically
 169 examine how different model components (e.g. noise, network structure, baseline excitability,
 170 coupling strength) impact the propensity of seizure-like activity. Full details of model variables and
 171 parameters are provided in Tables 1 and 2.
 172

Variable	Interpretation	Dimension
z_j	Complex activity variable of node j	2 x N
λ_j	Excitability of node j	N
W_j	Complex Wiener process	2 x N

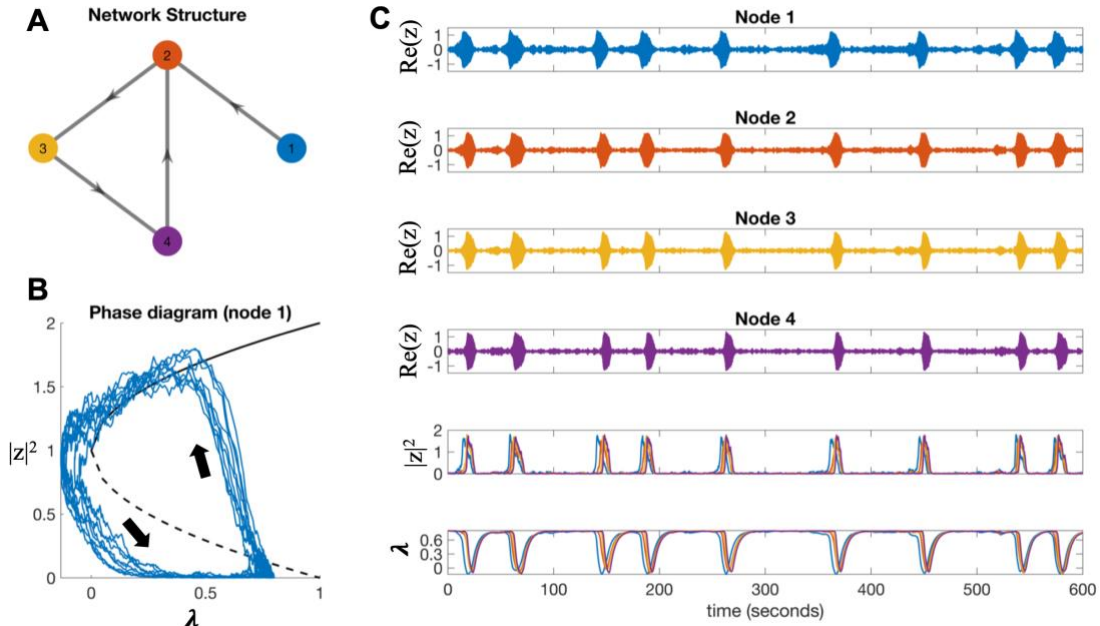
173 **Table 1:** Model variables.
 174

Parameter	Interpretation	Typical range	Value
N	Number of nodes in the network	3-10	4
ω	Frequency of the stable limit cycle	3-50	20
β	Coupling strength between nodes	0.05-6	-
α	Noise strength	0.005-0.10	0.08
τ	Time-scale of the slow variable λ	5-50	5
λ_{j0}	Baseline level of excitability	$\in [0,1]$	0.75
A	Adjacency matrix	1 (connection), 0 (no connection)	-

175 **Table 2:** Model parameter values³³.
 176

177 An example of the dynamics observed in a network with 4 nodes is shown in Fig. 1. The phase diagram
 178 (Fig. 1B) shows that the system spends most of the time near the fixed point $z = 0$. In this regime the
 179 simulated EEG activity ($Re(z_j)$) remains in the background state (low amplitude noisy oscillations on
 180 the panels on the right). Eventually, the trajectory crosses the boundary of the basin of attraction of the
 181 fixed point (dashed line) and transitions into the seizure-like state. A drop in the excitability variable

182 λ follows (see equation 2) and the system is brought back to the proximity of the fixed point (the
 183 background state).
 184



185
 186 **Fig. 1:** Example of network dynamics for a 4-node network. (A) Specific network structure. (B) Trajectory in phase
 187 space for node 1 (other nodes display similar patterns). The direction of the flow is anti-clockwise (see arrows). (C)
 188 simulated electrographic (e.g. EEG) activity ($Re(z_j)$) for the four nodes, amplitude of the complex activity variables
 189 ($|z_j|^2$), and slow excitability variables (λ_j). Note that all nodes transitioned simultaneously into the seizure-like state
 190 (synchronization). All simulations were carried with an Euler-Maruyama scheme with $dt = 0.0001$. See Table 2 for
 191 default values for the model parameters.

192
 193 For certain classes of coupled bistable systems with noise-induced transitions, it is possible to
 194 analytically examine the behaviours of these systems, for example, derive analytical expressions for
 195 the escape time using the Eyring-Kramer equation^{34,35}. These escape times have been shown to
 196 correlate with seizure propensity^{22,36}. In general, however, these high-dimensional dynamic network
 197 models do not allow for such analytical treatment and numerical simulations can provide insight into
 198 how different mechanisms contribute to seizure propensity.

200 B. Brain Network Ictogenicity

201
 202 Recently, several works have used the concept of *Brain Network Ictogenicity (BNI)* to estimate the
 203 propensity of a network to generate what we term seizure-like activity^{36,37}. For example identifying
 204 optimal resection regions in epilepsy brain surgery^{26,27,30}, to classify focal and generalized epilepsies³⁹,
 205 and to assess lateralization in focal epilepsy⁴⁰.

206
 207 Broadly speaking, *BNI* can be thought of as the proportion of time that nodes within a network spend
 208 in a seizure-like state. The propensity of seizure-like activity critically depends on the interplay
 209 between a number of model parameters. In particular the coupling strength (β), noise strength (α), the
 210 time-constant of the slow variable (τ), the network topology (for example, whether it is strongly or
 211 weakly connected, the presence of cycles) and the baseline excitability (λ_{j0}). For example, if the
 212 baseline excitability λ_{j0} is close to 0, low values of noise strength α are unlikely to lead to seizures
 213 whereas if λ_{j0} is close to 1, the same strength of noise would lead to several seizures. In practice the
 214 calculation of *BNI* can be implemented in several different ways and depends on many factors,
 215 including the specific dynamical model, the precise definition of what characterizes a seizure in this

216 system, the details of the state transition, model parameters, and coupling type, amongst others.
 217 Despite these many factors, the value of BNI calculated using different models is often similar^{30,32}.

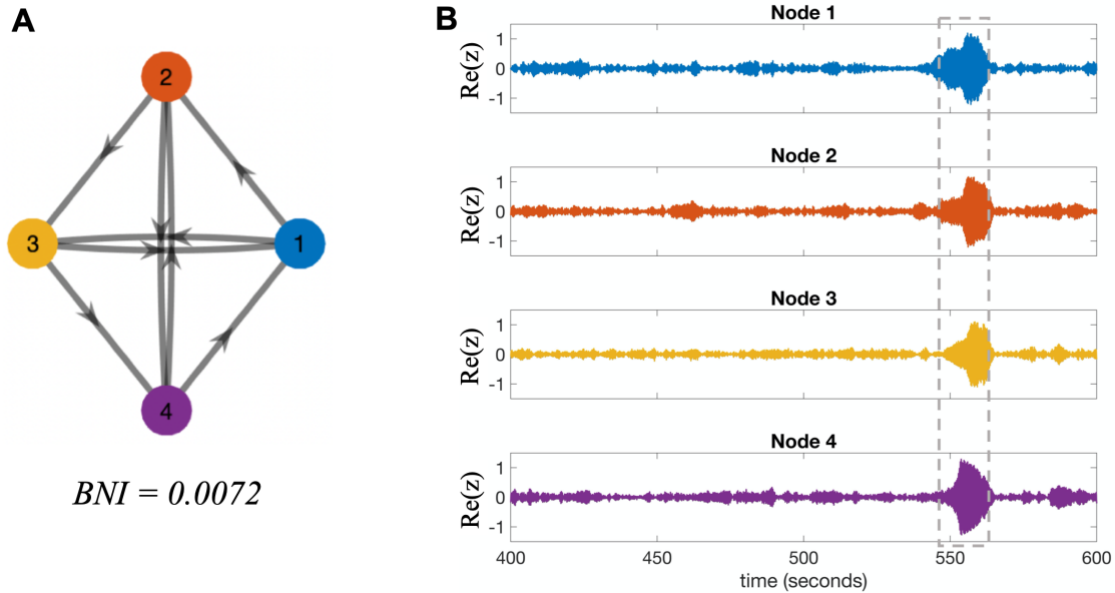
218
 219 An important consideration when calculating BNI is to define what constitutes a seizure within the
 220 context of the model. For the model we consider, there are two stable attractors, which correspond to
 221 a background state and a seizure-like state, and therefore we can use the separatrix as a threshold for
 222 whether a node is in the seizure-like state. The details on how such a threshold is defined are often
 223 omitted, in spite of the fact that this threshold often has an influence on the absolute values of the BNI .

224
 225 In this study we are primarily interested in the effect of the network structure on seizure propensity,
 226 we focus on when seizure-like activity across multiple nodes is driven by the connectivity between
 227 them. Consequently, the BNI for a given dynamic network structure is quantified by evaluating how
 228 long two or more nodes are simultaneously in the seizure-like state (this means that if a single
 229 individual node is in the seizure-like state whilst the other $N - 1$ nodes are in the background state,
 230 we do not consider this to be a seizure).

231
 232 To quantify the BNI for a given simulation of the dynamic network model, we start by finding all
 233 segments in the simulation where at least two nodes are simultaneously in the high-amplitude seizure-
 234 like state ($|z_j|^2 > 0.5$). The BNI is defined as the total sum of the lengths of these segments, scaled
 235 by $m/(T_s N)$, where m is the number of nodes in the seizure-like state in each segment ($m \geq 2$), T_s
 236 is the total simulation time and N is the total number of nodes.

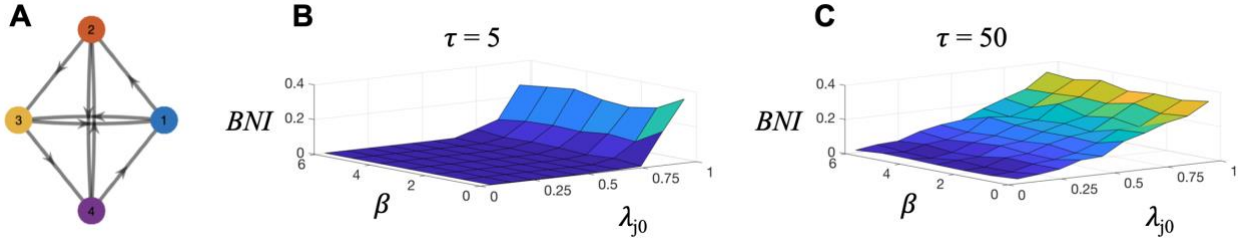
237
 238 Consequently, it holds that $BNI \in [0,1]$, where a value of 0 means there was no synchronised seizure-
 239 like activity in the simulation, whereas a value of 1 means that all nodes were in the seizure-like state
 240 for the entire simulation. See Fig. 2 for a simple example of how the BNI is calculated for a given
 241 dynamic network model.

242



243
 244 **Fig. 2:** The BNI calculated for a four-nodes network. (A) directed, unweighted network consisting of four nodes. (B)
 245 simulated electrographic recording. This simulation contained one segment for which at least 2 nodes have $|z_j(i)|^2 > 0.5$
 246 (dotted box at approximately 550 seconds). Model simulation with: $\beta = 0.20$, $T_s = 1000$; Euler-Maruyama scheme
 247 with $dt = 0.0001$; initial conditions: $z_j(0) \approx 0$ and $\lambda_j(0) \approx \lambda_{j0}$, for all other default values see Table 2.
 248

249 Systematic explorations of the key parameters allow one to extend the *BNI* as a high-dimensional
 250 integral for a given network structure. Fig. 3 shows the dependence of seizure propensity to the choice
 251 of parameters of the dynamic network model. Even though small changes in parameter values seem to
 252 lead to smooth, monotonic changes in the *BNI*, this suggests it is in general important to consider the
 253 certainty of parameter inference in networks of dynamic models as this could significantly impact the
 254 higher-level model outputs of interest.
 255



256
 257 **Fig. 3:** Seizure propensity (as quantified by *BNI*) depends on the coupling strength β , baseline excitability λ_{j0} and the
 258 slow time-scale τ . The *BNI* landscape computed for a given network structure (A) for different values of β and λ_{j0} . (B)
 259 $\tau = 5$; (C) $\tau = 50$. All simulations with total simulation time: $T_s = 1000$, using an Euler-Maruyama scheme with $dt =$
 260 0.0001 ; $\alpha = 0.08$. Initial conditions: $z_j(0) \approx 0$ and $\lambda_j(0) \approx \lambda_{j0}$.
 261

262 C. Perturbations to network structure

263
 264 To explore the effect of changes to network topology, such as the removal of a node or the addition or
 265 removal of an edge, we start with network structures with four nodes. Initially, we only consider
 266 network structures that are at least weakly connected, which guarantees there are no disconnected
 267 nodes or subgraphs. If a network perturbation renders the network disconnected, the *BNI* of the
 268 perturbed network is determined by the connected component with the largest *BNI*.
 269

270 In order to consider all potential types of behaviour for a given network structure, we do not restrict
 271 our analysis to a single value of the coupling parameter. The *BNI* is averaged over a wide range of
 272 values for β (see Table 2), covering all from weak to strong coupling relative to noise and excitability.
 273 Additionally, in this work we are not concerned with absolute values of the seizure propensity, which
 274 can be influenced by the baseline excitability (λ_{j0}), the timescale of the slow variable (τ), or the noise
 275 (α); but with the difference between the *BNI* before and after a network is perturbed, either by a node
 276 removal or by network reconfiguration. Therefore, a consistent choice for these parameters is sufficient
 277 to reveal the influence of network perturbations in seizure propensity. For the choices of fixed
 278 parameters please see Table 2.
 279

281 III. Results

282
 283 To understand the impact on network ictogenicity of virtual resections, and how this is further
 284 impacted by continued reorganization of the remaining network, we begin by performing a systematic
 285 analysis of networks with four nodes. We first establish the relationship between network structure
 286 and *BNI* for the given choice of fixed parameters in Table 2. We use this understanding to measure the
 287 change in *BNI* upon removal of individual nodes within different network structures, focussing on
 288 cases where the original network has high *BNI*. This focus is motivated by the potential clinical
 289 application, where such networks might be potentially suitable for surgical intervention. The impact
 290 of ongoing network reorganisation post virtual resection is evaluated by considering all possible
 291 individual edge changes in an exemplar network. We find examples where removal of a node results
 292 in a network with low *BNI* – the desired outcome – however, creating or removing individual edges

293 results in a dramatic increase in BNI . Finally, we show how this effect can also manifest in larger
294 networks, more in line with brain networks obtained from clinical data.

295

296 **A. Network ictogenicity for 4-nodes networks**

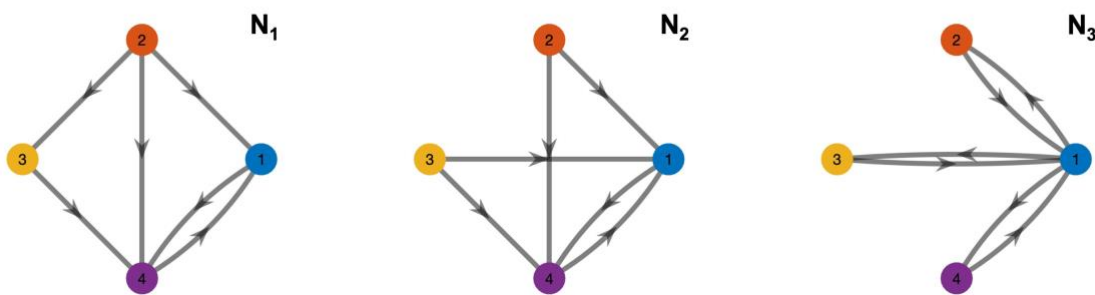
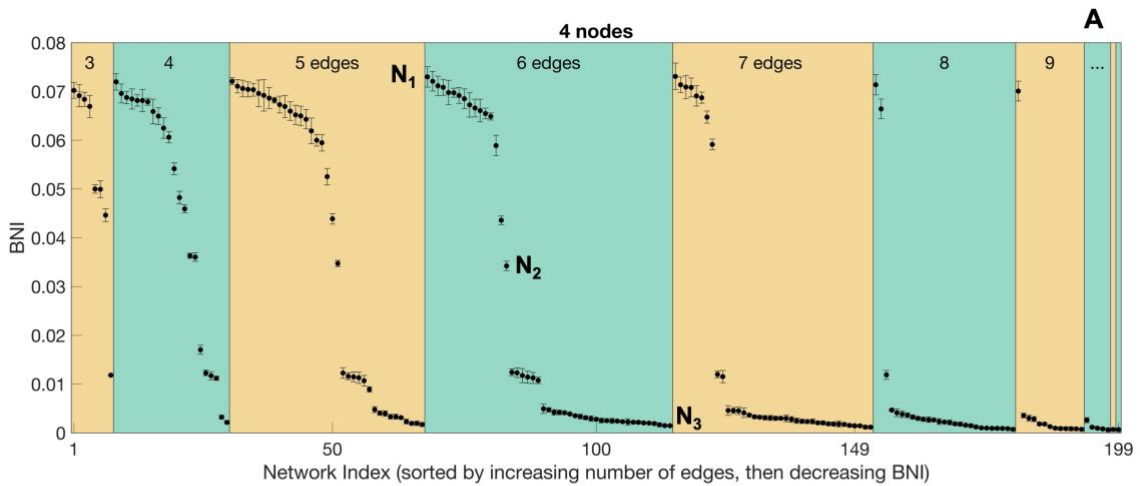
297

298 There are 199 non-isomorphic networks with four nodes that are weakly or strongly connected. In Fig.
299 4(A) we present calculations of the BNI where networks are sorted by increasing number of edges and,
300 within each edge group, by decreasing value of BNI . By comparing the BNI values for networks with
301 3 or 4 edges, and those with 10, 11 and 12 edges, we observe a tendency for networks to present, on
302 average, decreasing BNI as the number of edges in the network increases. For networks with 4 to 9
303 edges, the proportion of networks with relatively low values of BNI similarly grows with increasing
304 number of edges. This behaviour is due to the nature of the coupling between nodes within the network
305 (linear and proportional to the difference between node states), whereby a connection from node A to
306 node B results in node A influencing node B to behave in the same way. Combined with node dynamics
307 being brought back to the background state with time-scale τ following transition to the seizure-like
308 state, this makes network nodes hold themselves more strongly in the background state when there are
309 more connections within a network.

310

311 However, it is important to recognise that BNI does not decrease monotonically with increasing
312 number of edges. Rather, the effect of the network topology, and the hierarchy of the network in
313 particular, plays an important role. Interestingly, all edge groups in Fig. 4(A) present a similar pattern
314 on how the BNI decreases. Within each group, networks with relatively high BNI are those with a
315 single "driving" node (e.g. a node with no in-connections). An example of such a network is presented
316 in panel N_1 of Fig. 4 (6-edges network with highest BNI). In this example, node 2 is not being
317 influenced to remain in the background state by any other nodes, and when it transits to the seizure-
318 like state, it forces nodes 1, 3 and 4 to the same state, leading to a relatively high seizure propensity.
319 The network in panel N_2 considers a case with two driver nodes (2 and 3) which are connected to nodes
320 1 and 4. Nodes 2 and 3 have a similar influence here as node 2 in network N_1 . When both nodes transit
321 to the seizure-like state together, they force nodes 1 and 4 to the same state. However, in the case
322 where one node is in the seizure-like state and the other remains in the background state, they exert
323 opposite influences upon nodes 1 and 4. This competition leads to intermediate values of BNI for
324 networks with this general structure. Finally, network in panel N_3 is strongly connected and all nodes
325 tend to hold each other in the background state, resulting in low values of BNI .

326



327

328

329

330

331

332

333

334

335

336

337

338

339

340

341

342

343

344

345

346

347

348

349

350

351

352

353

354

Fig. 4: (A) *BNI* for all networks with 4 nodes, sorted first by increasing number of edges (between 3 and 12), then by decreasing *BNI*. Exemplar 6-edges networks are presented for high (N_1), intermediate (N_2) and low (N_3) values of *BNI*. Error bars represent variations due to noise.

B. Effects of node removal

Epilepsy surgery aims to reduce seizure propensity through the removal of cortical tissue considered key to generating seizures⁴¹. Within the context of our dynamic network model, we explore this through systematic removal of individual nodes and studying the impact on the level of *BNI* as a result. Nodes identified as being essential to the emergence and/or spreading of seizure-like activity would represent the best candidates for surgical resection. It is important to note on the other hand that some nodes may influence emergent dynamics in such a way as to prevent the spread of seizures, and the removal of such nodes might lead to even more seizures.

To consider these issues Fig. 5(A) illustrates the distribution of *BNI* before and after the removal of each node individually for a given four-node network. The diagonal line separates the cases where the *BNI* after node removal is smaller than before (blue region) from the cases where a removal leads to a remaining network with higher *BNI* (red region). The networks clustered on the left side of the figure have a low *BNI* and any intervention either leads to a similar or higher *BNI*. On the opposite side, networks with high *BNI* are those potential candidates for node removal in order to try to reduce the overall seizure propensity. However, not all networks can lead to lower *BNI* by node removal. From the 58 networks clustered in the region of high *BNI* before node removal ($BNI > 0.055$), 37 (63.8%) have at least one node removal that leads to a network with significantly lower ictogenicity ($BNI < 0.020$). From the 232 possible node removals (58 networks \times 4 nodes), only 45 (19.4%) lead to a significant reduction in *BNI*.

355 Two exemplar networks with high *BNI* are shown in Fig. 5 (N_1 and N_2). The removal of nodes 1, 3 or
356 4 in the network in N_1 lead to networks with *BNI* very similar to the complete network. However, the
357 removal of node 2 (a driver node) leads to a significant reduction in *BNI*. From a model perspective,
358 this would represent a suitable candidate for therapeutic resection for controlling seizure activity.
359 Conversely, network N_2 also have a relatively high *BNI*, however in this case no node removal lead to
360 a substantial reduction in *BNI*. Here, node removal is not an efficient alternative to reduce network
361 ictogenicity.

362

363 **C. Robustness to connectivity changes**

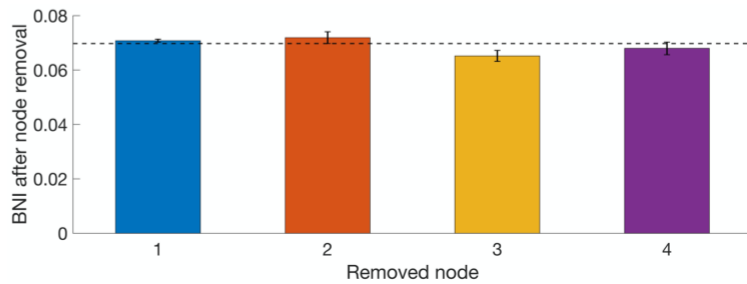
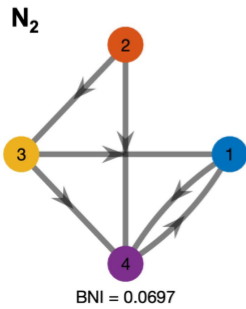
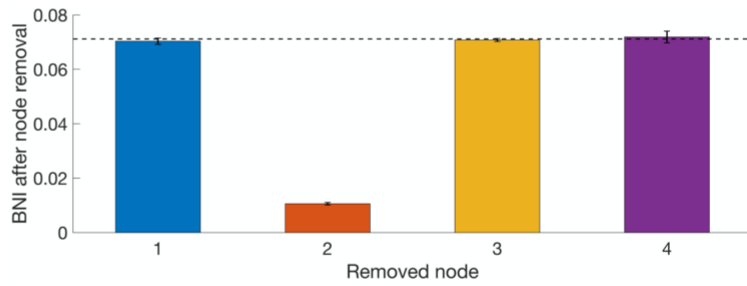
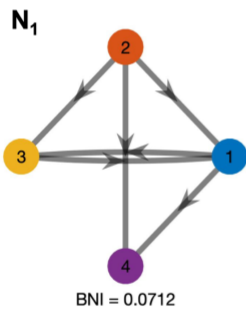
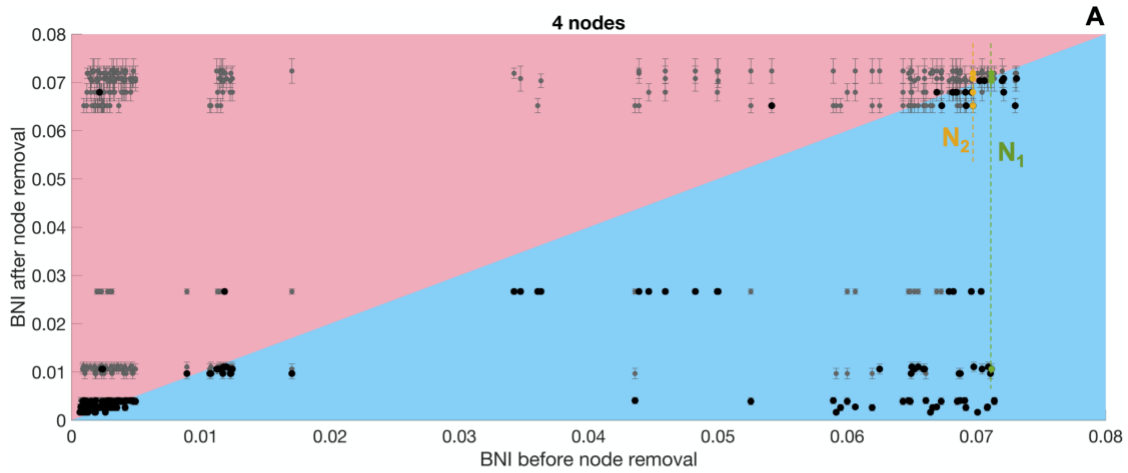
364

365 A critical question to consider is the impact of ongoing network reorganisation following the removal
366 of a node or nodes within the network. Effectively, this is an issue of robustness of a network with
367 respect to increases in *BNI* when edges are either added or removed. To consider this, we evaluate the
368 effect of all possible configurations involving adding or removing a single edge in the remaining
369 network. In Fig. 6 we present an example where network reconfiguration post-removal of a node has
370 a dramatic influence on the level of *BNI*.

371

372 The starting network presented in Fig. 6(A) has a relatively high *BNI*. As shown in Fig. 6(B), removing
373 nodes 2, 3 or 4 do not result in a significant change in *BNI*. On the other hand, the removal of node 1,
374 which results in the network presented in panel C of the same figure, significantly reduces *BNI*,
375 suggesting this is a suitable candidate for therapeutic intervention. However, if we add or remove a
376 single edge in the remaining network, which would lead to one of the networks presented in panels D,
377 E and F (all other possible combinations are isomorphic to one of these networks), the *BNI* increases
378 to levels similar to those observed prior to node removal (network in panel A).

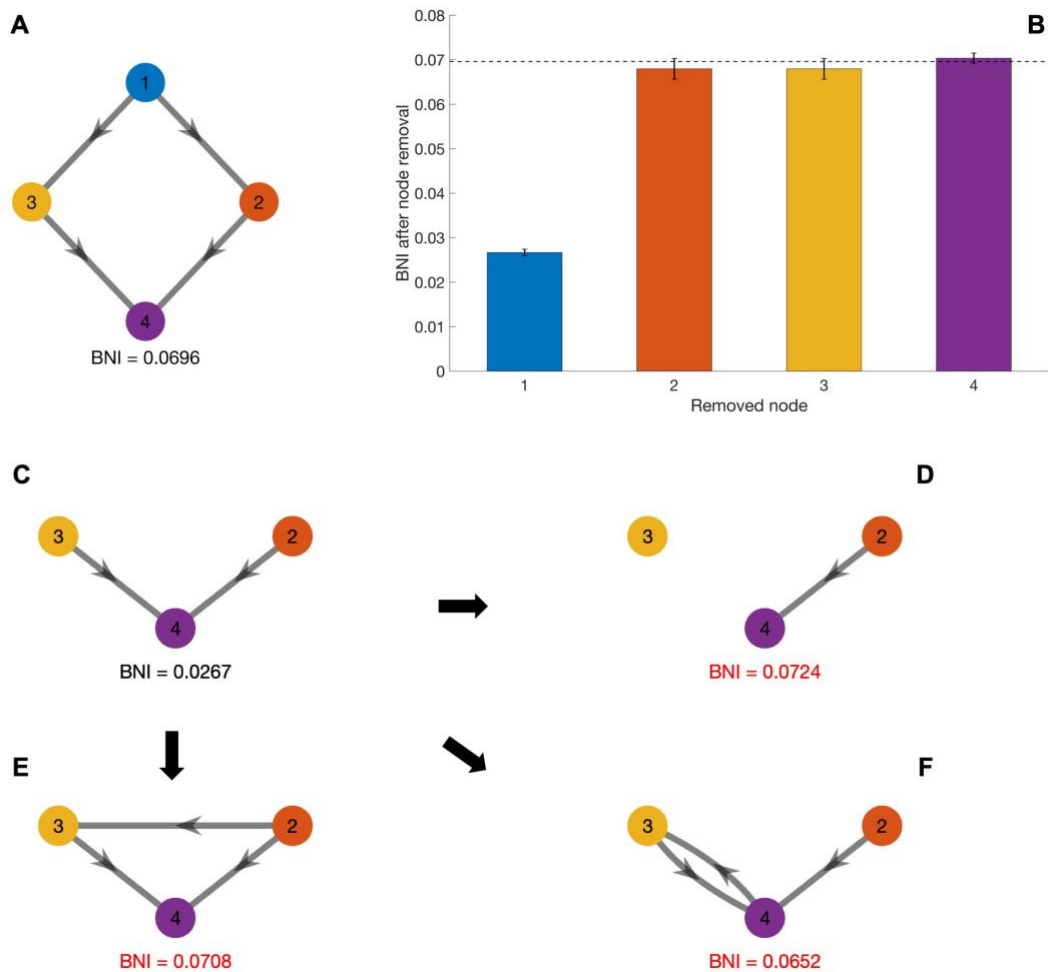
379



380
 381 **Fig. 5:** (A) *BNI* before and after all possible node removal (four one-node removal). Minimum *BNI* after node
 382 removal is shown in black, others are shown in light grey. Region in blue (red) indicate a decrease (increase) in *BNI* after
 383 node removal. (N_1 and N_2) Exemplar networks of high *BNI*, with the respective values of the *BNI* after node removal for all
 384 nodes individually. Dashed lines represent *BNI* before node removal. The dots associated to networks N_1 and N_2 in panel
 385 A are shown in green and yellow, respectively.

386
 387 This effect is due to the fact that after node 1 was removed, the remaining network has two "competing
 388 drivers", similar to the situation described in Fig. 5(N_2). This competing influence results in a lower
 389 value of the *BNI*, however this configuration is quite unstable. The addition or removal of any edge
 390 breaks up the symmetry between the competing elements and a single driver takes over, bringing the
 391 *BNI* up again.

392
 393



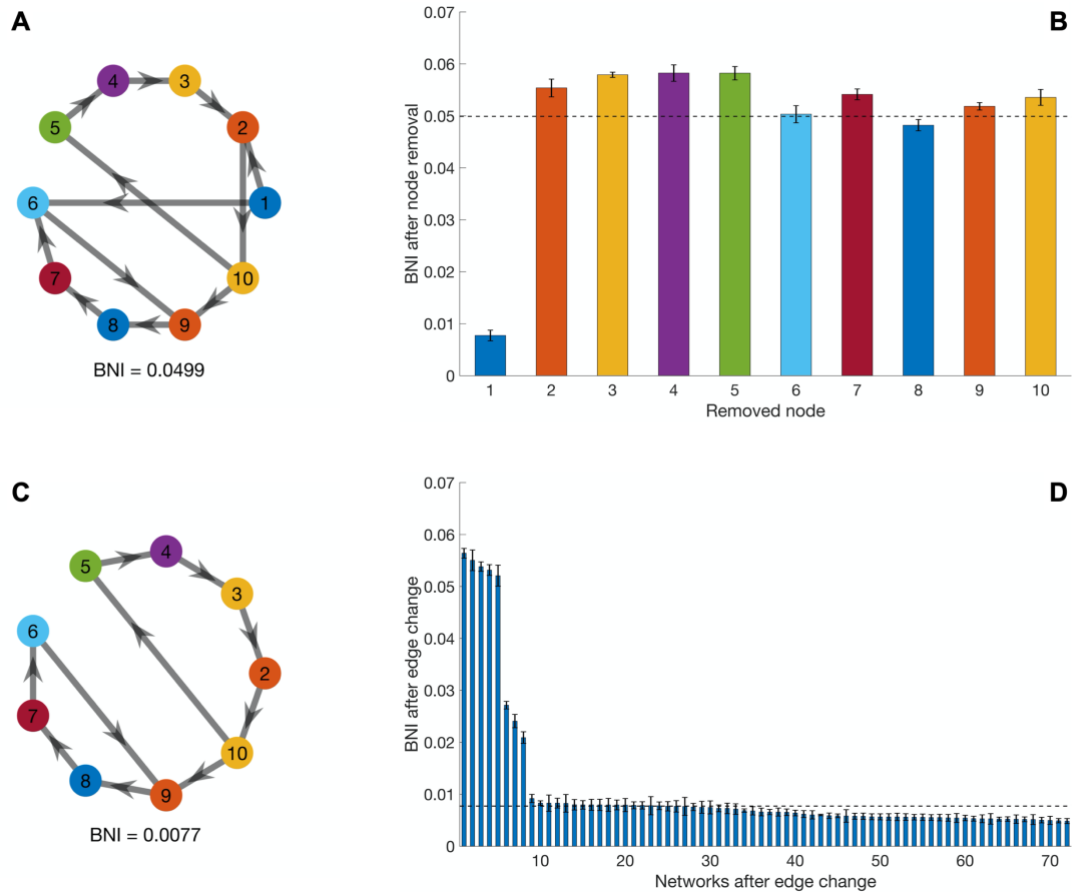
394
 395
 396
 397
 398
 399
 400
 401
 402
 403
 404
 405
 406
 407
 408
 409
 410
 411
 412
 413
 414
 415
 416
 417

Fig. 6: (A) Exempler network with 4 nodes. (B) *BNI* for the resulting networks after the removal of each of the 4 nodes individually (dashed line represents *BNI* before node removal). (C) Resulting network after the removal of node 1 (node removal that leads to the lowest *BNI*). (D, E and F) Resulting networks after removing or adding one edge in the network in (C), evidencing a clear increase in the *BNI*.

D. Evaluation of lager networks

This effect is not an artefact resulting from small network sizes. In Fig. 7 we find similar effects in a network of 10 nodes: a size more in line with the typical network sizes obtained from scalp, stereo or intracranial EEG⁴². The network presented in Fig. 7(A) has a relatively high *BNI*. The effects of removing all nodes individually are presented in Fig. 7(B), and it suggests that only the removal of node 1 leads to a significant reduction in the *BNI*. The network resulting from removing node 1 is presented in Fig. 7(C). This network is formed by two cycles, one involving nodes 2, 3, 4, 5 and 10, and the other by nodes 6, 7, 8, and 9. The cycles are connected by an edge between nodes 9 and 10. This network presents a relatively low *BNI*. However, if we probe the *BNI* stability by adding or removing individual edges, Fig. 7(D) shows that for over 10% of the resulting networks the *BNI* increases significantly, sometimes to values even higher than before the removal of node 1.

These findings are a potentially important consideration for pre-surgical planning. A strategy that a priori leads to a substantial reduction in *BNI* can result in a remaining network that is prone to a return to high seizure propensity with only a few connections added or removed.



418
419

420 **Fig. 7:** (A) Exemplar network with 10 nodes. (B) BNI for the resulting networks after the removal of each of the 10
421 nodes individually (dashed line represents BNI before node removal). (C) Resulting network after the removal of node 1
422 (node removal that leads to the lowest BNI). (D) BNI for all 72 possible networks obtained by removing or adding one
423 edge in the network in (C), sorted by decreasing BNI (dashed line represents BNI before edge change). Note that 8
424 networks (>10%) present a significant increase in the BNI .

425
426

427 IV. Discussion

428

429 In this paper we used a canonical dynamic network model to explore seizure propensity in brain
430 networks. We showed that due to the interplay of coupling between brain regions and the excitability
431 within brain regions, a decrease in BNI is correlated with an increased number of edges within the
432 network. We further showed that the hierarchy of the network plays a crucial role in the level of BNI :
433 the presence of a single driving node leads to high values of BNI , competing driver nodes typically
434 result in intermediate levels of ictogenicity, whilst strongly connected networks tend to present very
435 low ictogenicity.

436

437 Building on these observations, we systematically evaluated how removal of network nodes influences
438 the ictogenicity of the remaining network. These so-called virtual resections are effectively an *in silico*
439 proxy for brain surgery, enabling the relative merits of alternative surgical strategies to be evaluated.
440 Of particular importance is the robustness of an intervention to future evolution of the remaining
441 network. To investigate this, we systematically studied the impact on BNI of adding or removing edges
442 within a network for which a node had been previously removed. We found networks for which
443 initially high BNI was significantly reduced upon removal of a specific node. However, any alterations
444 to the remaining network led to a return to high levels of BNI , similar to those prior to node removal.

445

446 A potential limitation of our study is that *BNI* is agnostic to seizure-frequency: a simulation in which
447 all nodes enter the seizure-like state for 20 seconds has the same *BNI* as a simulation in which all
448 nodes enter the seizure-like state ten times for 2 seconds each. In addition, identical values of *BNI*
449 can be achieved through different mechanisms and patterns of activity. However, in contexts where
450 the differentiation between specific seizure patterns are important, the *BNI* framework described in
451 this work can be extended. For example, Lopes *et al.*³⁹ have used the average slope of the *BNI* as a
452 function of the coupling strength (what the authors called the *Ictogenic Spread*) to classify genetic
453 generalized epilepsy versus mesial temporal lobe epilepsy. Woldman *et al.*⁴³ introduced two
454 measures: the onset index and the participation index that incorporate the level of synchronised
455 activity within brain regions and the ability of those brain regions to either drive seizure onset, or to
456 become involved in such activity. Furthermore, these potential limitations are likely to be context
457 dependent. For example, people with epilepsy may place high value on measuring the number of
458 seizures they experience, whilst the total duration of those events is less important. On the other
459 hand, a neurosurgeon planning surgery, will primarily be concerned with how a specific resection
460 will affect a given, baseline, seizure propensity. We finally note that the results of our work are not
461 impacted by these limitations, since we are interested in seizure susceptibility more generally,
462 independent of any specific activity patterns.

463

464 Taking into account the robustness of a perturbed network to subsequent alterations to its connectivity
465 is an important consideration in pre-surgical planning. For example, there may be competing strategies
466 which result in an initial reduction in seizure propensity. However, one is more sensitive to subsequent
467 network alterations than the other. Therefore, an important next step for this research is the application
468 of these theoretical concepts to networks inferred directly from clinical data. This would provide the
469 opportunity to better characterise long-term seizure freedom, given an apparently successful surgical
470 intervention.

471

472 **Acknowledgments**

473 LJ and JRT acknowledge financial support from the EPSRC via grant EP/N014391/1. LJ, WW and
474 JRT acknowledge financial support from Innovate UK via grant TS/R00546X/1. WW acknowledges
475 financial support from the MRC (MR/N01524X/1) and from Epilepsy Research UK (F2002). WW and
476 JRT are co-founders of Neuronostics.

477

478 The data that support the findings of this study are available from the corresponding author upon
479 reasonable request.

480

481 **References**

482

- 483 1. WHO | Epilepsy. *WHO* (2017).
- 484 2. Banerjee, P. N., Filippi, D. & Allen Hauser, W. The descriptive epidemiology of epilepsy-A
485 review. *Epilepsy Research* (2009).
- 486 3. Kwan, P. & Brodie, M. J. Early identification of refractory epilepsy. *N. Engl. J. Med.* (2000).
- 487 4. Fisher, R., Salanova, V., Witt, T., Worth, R., Henry, T., Gross, R., Oommen, K., Osorio, I.,
488 Nazzaro, J., Labar, D., Kaplitt, M., Sperling, M., Sandok, E., Neal, J., Handforth, A., Stern, J.,
489 DeSalles, A., Chung, S., Shetter, A., *et al.* Electrical stimulation of the anterior nucleus of
490 thalamus for treatment of refractory epilepsy. *Epilepsia* (2010).
- 491 5. Duncan, J. S., Winston, G. P., Koepp, M. J. & Ourselin, S. Brain imaging in the assessment
492 for epilepsy surgery. *Lancet Neurol.* **15**, 420–433 (2016).
- 493 6. De Tisi, J., Bell, G. S., Peacock, J. L., McEvoy, A. W., Harkness, W. F., Sander, J. W. &
494 Duncan, J. S. The long-term outcome of adult epilepsy surgery, patterns of seizure remission,

- 495 and relapse: A cohort study. *Lancet* **378**, 1388–1395 (2011).
- 496 7. Mohan, M., Keller, S., Nicolson, A., Biswas, S., Smith, D., Farah, J. O., Eldridge, P. &
497 Wiesmann, U. The long-term outcomes of epilepsy surgery. *PLoS One* (2018).
- 498 8. Sheikh, S. R., Kattan, M. W., Steinmetz, M., Singer, M. E., Udeh, B. L. & Jehi, L. Cost
499 effectiveness of surgery for drug resistant temporal lobe epilepsy in the US. *Neurology* (2020).
- 500 9. Engel, J. Surgery for Seizures. *N. Engl. J. Med.* (1996).
- 501 10. Engel, J. J. The current place of epilepsy surgery. *Curr. Opin. Neurol.* (2017).
- 502 11. Kramer, M. A. & Cash, S. S. Epilepsy as a Disorder of Cortical Network Organization.
503 *Neurosci.* **18**, 360–372 (2012).
- 504 12. Richardson, M. P. Large scale brain models of epilepsy: dynamics meets connectomics. *J.*
505 *Neurol. Neurosurg. Psychiatry* **83**, 1238–1248 (2012).
- 506 13. Van Diessen, E., Diederer, S. J. H., Braun, K. P. J., Jansen, F. E. & Stam, C. J. Functional and
507 structural brain networks in epilepsy: What have we learned? *Epilepsia* (2013).
- 508 14. Geier, C. & Lehnertz, K. Long-term variability of importance of brain regions in evolving
509 epileptic brain networks. *Chaos* (2017).
- 510 15. Li Hegner, Y., Marquetand, J., Elshahabi, A., Klamer, S., Lerche, H., Braun, C. & Focke, N.
511 K. Increased Functional MEG Connectivity as a Hallmark of MRI-Negative Focal and
512 Generalized Epilepsy. *Brain Topogr.* (2018).
- 513 16. van Mierlo, P., Höller, Y., Focke, N. K. & Vulliemoz, S. Network Perspectives on Epilepsy
514 Using EEG/MEG Source Connectivity . *Frontiers in Neurology* vol. 10 721 (2019).
- 515 17. Fisher, R. S., Cross, J. H., French, J. A., Higurashi, N., Hirsch, E., Jansen, F. E., Lagae, L.,
516 Moshé, S. L., Peltola, J., Roulet Perez, E., Scheffer, I. E. & Zuberi, S. M. Operational
517 classification of seizure types by the International League Against Epilepsy: Position Paper of
518 the ILAE Commission for Classification and Terminology. *Epilepsia* (2017).
- 519 18. Stam, C. J. Modern network science of neurological disorders. *Nature Reviews Neuroscience*
520 (2014).
- 521 19. Woldman, W. & Terry, J. R. Multilevel Computational Modelling in Epilepsy: Classical
522 Studies and Recent Advances. in *Validating Neuro-Computational Models of Neurological*
523 *and Psychiatric Disorders* (eds. Bhattacharya, B. S. & Chowdhury, F. N.) 161–188 (2015).
- 524 20. Terry, J. R., Benjamin, O. & Richardson, M. P. Seizure generation: The role of nodes and
525 networks. *Epilepsia* **53**, (2012).
- 526 21. Kalitzin, S. N., Velis, D. N. & Lopes da Silva, F. H. Stimulation-based anticipation and
527 control of state transitions in the epileptic brain. *Epilepsy Behav.* (2010).
- 528 22. Benjamin, O., Fitzgerald, T. H., Ashwin, P., Tsaneva-Atanasova, K., Chowdhury, F.,
529 Richardson, M. P. & Terry, J. R. A phenomenological model of seizure initiation suggests
530 network structure may explain seizure frequency in idiopathic generalised epilepsy. *J. Math.*
531 *Neurosci.* **2**, 1 (2012).
- 532 23. Milton, J. & Jung, P. *Epilepsy as a Dynamic Disease*. (Springer Berlin Heidelberg, 2003).
- 533 24. Moraes, M. F. D., de Castro Medeiros, D., Mourao, F. A. G., Cancado, S. A. V. & Cota, V. R.
534 Epilepsy as a dynamical system, a most needed paradigm shift in epileptology. *Epilepsy and*
535 *Behavior* (2019).
- 536 25. Hutchings, F., Han, C. E., Keller, S. S., Weber, B., Taylor, P. N. & Kaiser, M. Predicting
537 Surgery Targets in Temporal Lobe Epilepsy through Structural Connectome Based
538 Simulations. *PLoS Comput. Biol.* (2015).
- 539 26. Goodfellow, M., Rummel, C., Abela, E., Richardson, M. P., Schindler, K. & Terry, J. R.
540 Estimation of brain network ictogenicity predicts outcome from epilepsy surgery. *Sci. Rep.* **6**,
541 29215 (2016).
- 542 27. Sinha, N., Dauwels, J., Kaiser, M., Cash, S. S., Westover, M. B., Wang, Y. & Taylor, P. N.
543 Predicting neurosurgical outcomes in focal epilepsy patients using computational modelling.
544 *Brain* **140**, 319–332 (2016).

- 545 28. Khambhati, A. N., Davis, K. A., Lucas, T. H., Litt, B. & Bassett, D. S. Virtual Cortical
546 Resection Reveals Push-Pull Network Control Preceding Seizure Evolution. *Neuron* (2016).
- 547 29. Jirsa, V. K., Proix, T., Perdikis, D., Woodman, M. M., Wang, H., Bernard, C., Bénar, C.,
548 Chauvel, P., Bartolomei, F., Bartolomei, F., Guye, M., Gonzalez-Martinez, J. & Chauvel, P.
549 The Virtual Epileptic Patient: Individualized whole-brain models of epilepsy spread.
550 *Neuroimage* **145**, 377–388 (2017).
- 551 30. Lopes, M. A., Richardson, M. P., Abela, E., Rummel, C., Schindler, K., Goodfellow, M. &
552 Terry, J. R. An optimal strategy for epilepsy surgery: Disruption of the rich-club? *PLoS*
553 *Comput. Biol.* (2017).
- 554 31. Johnston, M. V. Clinical disorders of brain plasticity. *Brain and Development* (2004).
- 555 32. Junges, L., Lopes, M. A., Terry, J. R. & Goodfellow, M. The role that choice of model plays
556 in predictions for epilepsy surgery. *Sci. Rep.* **9**, 7351 (2019).
- 557 33. Hebbink, J., Meijer, H., Huiskamp, G., van Gils, S. & Leijten, F. Phenomenological network
558 models: Lessons for epilepsy surgery. *Epilepsia* **58**, e147–e151 (2017).
- 559 34. Neiman, A. Synchronizationlike phenomena in coupled stochastic bistable systems. *Phys. Rev.*
560 *E* (1994).
- 561 35. MacKay, R. S. & Sepulchre, J. A. Multistability in networks of weakly coupled bistable units.
562 *Phys. D Nonlinear Phenom.* (1995).
- 563 36. Ashwin, P., Creaser, J. & Tsaneva-Atanasova, K. Fast and slow domino regimes in transient
564 network dynamics. *Phys. Rev. E* (2017).
- 565 37. Petkov, G., Goodfellow, M., Richardson, M. P. & Terry, J. R. A critical role for network
566 structure in seizure onset: A computational modeling approach. *Front. Neurol.* **5**, (2014).
- 567 38. Lopes, M. A., Junges, L., Woldman, W., Goodfellow, M. & Terry, J. R. The Role of
568 Excitability and Network Structure in the Emergence of Focal and Generalized Seizures.
569 *Front. Neurol.* (2020).
- 570 39. Lopes, M. A., Perani, S., Yaakub, S. N., Richardson, M. P., Goodfellow, M. & Terry, J. R.
571 Revealing epilepsy type using a computational analysis of interictal EEG. *Sci. Rep.* (2019).
- 572 40. Lopes, M. A., Junges, L., Tait, L., Terry, J. R., Abela, E., Richardson, M. P. & Goodfellow,
573 M. Computational modelling in source space from scalp EEG to inform presurgical evaluation
574 of epilepsy. *Clin. Neurophysiol.* (2020).
- 575 41. Rosenow, F. & Lüders, H. Presurgical evaluation of epilepsy. *Brain* **124**, 1683–1700 (2001).
- 576 42. Aminoff, M. J. *Aminoff's Electrodiagnosis in Clinical Neurology*. *Aminoff's Electrodiagnosis*
577 *in Clinical Neurology* (2012).
- 578 43. Woldman, W., Schmidt, H., Abela, E., Chowdhury, F. A., Pawley, A. D., Jewell, S.,
579 Richardson, M. P. & Terry, J. R. Dynamic network properties of the interictal brain determine
580 whether seizures appear focal or generalised. *Sci. Rep.* **10**, 7043 (2020).
- 581